European Polymer Journal 58 (2014) 226–232

Contents lists available at ScienceDirect

European Polymer Journal

journal homepage: www.elsevier.com/locate/europolj

Macromolecular Nanotechnology

Generation of nanocomposites based on (PMMA-*b*-PCL)-grafted Fe_2O_3 nanoparticles and PS-*b*-PCL block copolymer

Irati Barandiaran [a], Ariel Cappelletti [b], Miriam Strumia [b], Arantxa Eceiza [a], Galder Kortaberria [a,*]

[a] "Materials + Technologies Group", Universidad del Pais Vasco/Euskal Herriko Unibertsitatea, Plaza Europa 1, 20018 Donostia, Spain
[b] Facultad de Ciencias Químicas, Universidad de Córdoba, Haya de la Torre Esq. Medina Allende, 5000 Córdoba, Argentina

ARTICLE INFO

Article history:
Received 7 April 2014
Received in revised form 13 June 2014
Accepted 25 June 2014
Available online 14 July 2014

Keywords:
Magnetic nanoparticles
Block copolymer
Atomic force microscopy
Grafting

ABSTRACT

The aim of this work is to obtain a good dispersion of Fe_2O_3 magnetic nanoparticles into a PS-*b*-PCL diblock copolymer. For this purpose nanoparticles have been modified in their surface by grafting a PMMA-*b*-PCL block copolymer into their surface, after being silanized. The grafting process has been probed by infrared spectroscopy, thermogravimetric analysis and transmission electron microscopy. Once modified, nanoparticles have been dispersed into the block copolymer. Nanostructured lamellar morphology of the block copolymer after annealing process has not been affected by the presence of nanoparticles, as has been probed by atomic force microscopy. Furthermore, their dispersion into the matrix has been improved when compared with unmodified nanoparticles. Though during modification process small aggregates of nanoparticles surrounded by PMMA-*b*-PCL brushes have been formed, morphology has not been altered or disrupted. Modified nanoparticles have been mostly placed at the interfaces among PS and PCL domains.

© 2014 Elsevier Ltd. All rights reserved.

1. Introduction

Self-assembly of block copolymers can generate a rich variety of nanostructures depending on the nature of the blocks, molecular weight and composition, and processing characteristics. Microphase or nanophase separation at the mesoscopic scale is generated by the repulsion between blocks linked by covalent attachment. This materials could open a way to generate different nanostructures with applications in fields such as medicine [1], surfactant chemistry [2], quantum dots [3], microcapsules [4], nanowires [5] and magnetic storage media [6,7], among others. In that way, the incorporation of inorganic nanoparticles into nanophase-separated structures could enable to obtain nanocomposites with prominent features such as optic, electronic, and magnetic properties [8–10].

On the other hand, magnetic nanoparticles have received special attention due to its potential applications in many diverse fields such as ferrofluids, magnetic resonance imagining, biomedicine and drug delivery [11–14].

The control of nanoparticle dispersion and their placement into desired domains is the main goal of preparing nanocomposites based on block copolymers and nanoparticles that tend to form big aggregates. In order to overcome this problem, the use of surfactants [15] or functionalization of nanoparticle surface with polymeric brushes are the most common routes [11,16]. Different methods have been used for anchoring polymeric brushes in the surface of nanoparticles, such as *grafting to* [17], *grafting from* [11] or *grafting through* [18]. In the first method end-functionalized polymer reacts with the reactive sites on nanoparticle surface. In the *grafting from* method the polymer chains grow in situ from an initiator that has been previously anchored to nanoparticle surface. The last method consists on a surface copolymerization

* Corresponding author. Tel.: +34 943017171.
E-mail address: galder.cortaberria@ehu.es (G. Kortaberria).

http://dx.doi.org/10.1016/j.eurpolymj.2014.06.022
0014-3057/© 2014 Elsevier Ltd. All rights reserved.

through a covalently linked monomer in which the inorganic phase is incorporated inside polymer chains.

Functionalization of magnetic nanoparticles surface with copolymers is becoming an extended practice. In this way, Wang et al. [19] functionalized iron oxide nanoparticles with P(PEGMA)-*co*-PNIPAAm copolymer via surface charge transfer free radical polymerization, Zhou et al. [20] functionalized magnetic nanoparticles with PEGMA-*b*-PMMA via atom transfer radical polymerization (ATRP), while He et al. [21] functionalized magnetic nanoparticles with a novel water soluble triblock copolymer via copper mediated atom transfer radical polymerization.

In this work, Fe_2O_3 magnetic nanoparticles have been functionalized by grafting a poly(methyl methacrylate-*b*-ε-caprolactone) (PMMA-*b*-PCL) copolymer to their surface in order to better disperse them into a poly(styrene-*b*-caprolactone) (PS-*b*-PCL) block copolymer without breaking nanostructures generated by thermal annealing.

2. Experimental

2.1. Materials

Maghemite (Fe_2O_3) nanoparticles with a nominal size of 9 nm and a polydispersity of 1.08 were purchased from Integram Technologies. 3-aminopropyltryethoxysilane (APTS) was purchased from Sigma–Aldrich, with a purity of 99%. Poly(methyl methacrylate-*b*-ε-caprolactone) block copolymer with terminal chlorine group (*Cl*-PMMA-*b*-PCL) was synthesized by ATRP with a number average molecular weight of 21,500 g/mol (f_{PMMA} = 0.7 and f_{PCL} = 0.3) and a polydispersity of 1.35. Synthesis conditions can be found elsewhere [22]. Poly(styrene-*b*-ε-caprolactone) (PS-*b*-PCL) block copolymer (f_{PS} = 0.7 and f_{PCL} = 0.3) was purchased from Polymer Source, Inc. The number average molecular weights of PS and PCL blocks are 27,000 and 10,000 g/mol, respectively, with a polydispersity index of 1.25. Toluene and tetrahydrofuran purchased from Aldrich were used as solvents.

2.2. Nanoparticle modification

Nanoparticle modification was carried out in two steps: first silanization process and then PMMA-*b*-PCL copolymer grafting to the silanized surface.

2.2.1. Silanization process

Fe_2O_3 magnetic nanoparticles were first modified with 3-aminopropyltryethoxysilane (APTS). Scheme 1 shows the reaction of nanoparticles with silane. This reaction implies a nucleophilic attack of OH groups at nanoparticle surface to the Si atoms of APTS. Extradry toluene, APTS and nanoparticles were mixed under sonication at inert atmosphere for 3 h at room temperature. Nanoparticles were subsequently washed six times with THF and then dried *in vacuo* at 40 °C for a period of 2 days. 1:1, 1:2, 1:3 and 1:5 OH/APTS molar ratios were investigated and as the highest silane grafting density was obtained for 1:3 ratio (as it will be shown below with TGA measurements), nanoparticles modified with this ratio were subsequently used for copolymer grafting.

2.2.2. Grafting to process

The anchoring of block copolymer was done by *grafting to* method. The covalent linking among silanized nanoparticles and PMMA-*b*-PCL block copolymer (with terminal *Cl*-group) was carried out by an alkylation reaction of amine groups present at the surface of nanoparticles, as it can be seen in Scheme 2. Extradry toluene solution of silanized nanoparticles and block copolymer was prepared. Grafting reaction was carried out at room temperature for 6 h with reflux. Functionalized nanoparticles were then cleaned six times with THF by centrifugation and then dried *in vacuo* at room temperature for a period of two days. 8%, 11%, 15% and 22% copolymer/APTS molar ratios were investigated. The highest grafting density was obtained for 15%, as it will be shown below with TGA measurements.

2.3. PS-b-PCL/Fe_2O_3-g-(PMMA-b-PCL) nanocomposite preparation

Fe_2O_3-*g*-(PMMA-*b*-PCL) nanoparticles were first dispersed in toluene for 2 h by sonication. Then PS-*b*-PCL block copolymer was added to the solution and films were prepared by spin coating. Obtained films were annealed at different temperatures under vacuum, together with those films of block copolymer without nanoparticles, prepared under the same conditions. Nanocomposites with 2 and 5 wt% of nanoparticles were prepared. The effect of annealing temperature and nanoparticle addition and concentration were analyzed.

2.4. Characterization techniques

Brunauer–Emmet–Teller (BET) isotherms were obtained with an Autosorb-1 from Quantachrome. Samples were dried at 100 °C for 2 h in a vacuum oven. Nitrogen

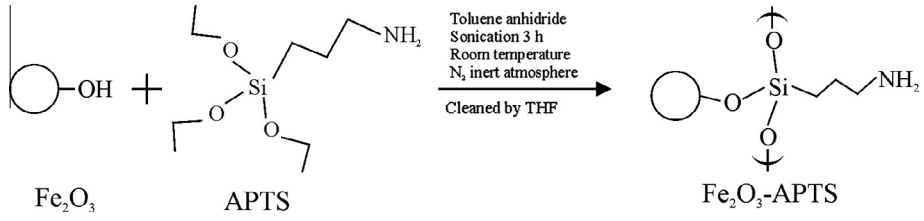

Scheme 1. Procedure used for Fe_2O_3 nanoparticle silanization.

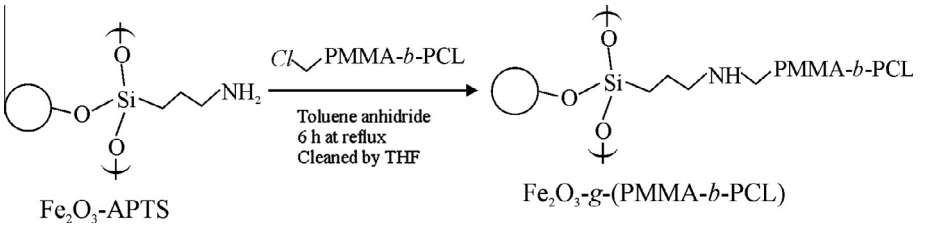

Scheme 2. Procedure used for grafting the block copolymer to the nanoparticles surface.

was used as the adsorbent, and all measurements took place at −196 °C.

Fourier transformed infrared spectroscopy (FTIR) was carried out with a Nicolet Nexus 600 FTIR spectrometer, performing 20 scans with a resolution of 4 cm^{-1}.

Thermogravimetric analysis was performed with a Mettler Toledo TGA/SDTA851 instrument. Tests were carried out from room temperature to 750 °C with a heating rate of 10 °C/min.

Nanoparticle size after modification was analized by transmission electron microscopy (TEM). A solution drop was deposited on a Formvard film Copper grid and examined in a Tecnai G2 20 Twin (FEI) microscope operating at an accelerating voltage of 200 keV in a bright-field image mode.

Morphologies obtained for different films were studied by atomic force microscopy by a scanning probe microscopy AFM Dimension ICON of Bruker, operating in tapping mode (TM–AFM). An integrated silicon tip/cantilever, from the same manufacturer, having a resonance frequency of around 300 kHz, was used. Measurements were performed at a scan rate of 1 Hz/s, with 512 scan lines.

3. Results and discussion

3.1. Fe_2O_3 nanoparticle characterization

The specific surface area of the nanoparticles measured with the BET method was estimated to be 102 m^2/g. The quantity of hydroxyl groups on the surface was determined with the use of TGA according to the method of Abbound et al. [23]. The surface density of hydroxyl groups was found to be 5.5 OH/nm^2. A typical FTIR spectrum of nanoparticles is shown in Fig. 1. The peak around 3400 cm^{-1} can be attributed to O–H bonds of nanoparticle hydroxyl groups. The other two peaks at 633 and 558 cm^{-1} are due to the Fe–O bond [24,25]. As it can be seen, there is a complete absence of any carbon-related peaks, this showing that nanoparticles were surfactant-free.

3.2. Fe_2O_3 nanoparticle silanization

The introduction of APTS onto nanoparticles is of crucial importance for further grafting of PMMA-*b*-PCL to the surface by the amino groups of silane. After modification, the amount of grafted silane was determined by TGA [26]. The surface density of the silane was about 1.9 molecules/nm^2. A direct comparison of the surface density of hydroxyl groups and that of the silane on the surface yielded a

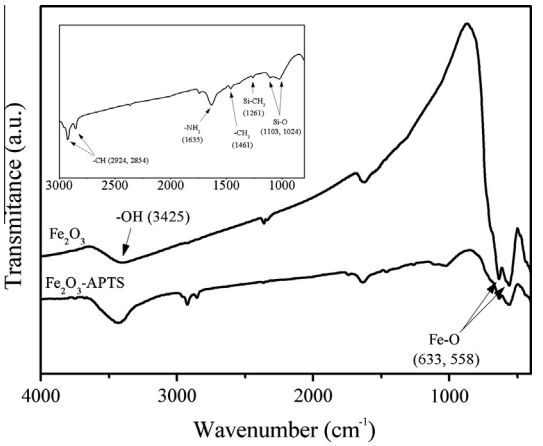

Fig. 1. FTIR spectra of neat and silanized Fe_2O_3 nanoparticles. Main bands are indicated by arrows. Inner spectrum shows a magnification of modified nanoparticle spectrum.

reaction efficiency of 35.8%. Those data were measured for nanoparticles modified with 1:3 OH/APTS molar ratio, which gave the highest silane density and efficiency when compared with other ratios used. For this reason, 1:3 ratio was chosen as the most efficient for nanoparticle silanization in our case. Fig. 1 shows FTIR spectrum of silanized nanoparticles together with that corresponding to pristine nanoparticles. The reaction between the hydroxyl groups

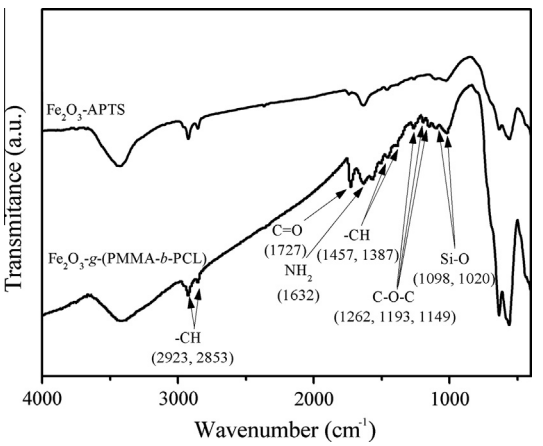

Fig. 2. FTIR spectra of silanized and PMMA-*b*-PCL-grafted nanoparticles. Main bands are indicated by arrows.

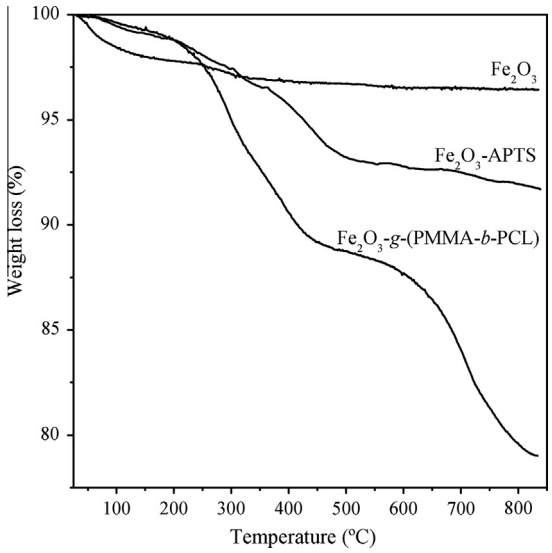

Fig. 3. TGA thermograms of unmodified, silanized and grafted Fe_2O_3 nanoparticles.

and APTS was confirmed by FTIR. Characteristic absorption bands of the aminopropyl groups, as well as the stretching vibration of Fe–O and Si–O bonds can be seen, together with the bands related to aliphatic C–H bonds [27], confirming the success of silanization process.

3.3. PMMA-b-PCL grafting

Fig. 2 shows FTIR spectra of nanoparticles grafted with PMMA-*b*-PCL copolymer. As it can be seen, the presence of the band related to the stretching vibrations of carbonyl group and that corresponding to COC single bond stretching deformation vibration, present in both PMMA and PCL blocks, suggest that copolymer has been grafted to the silanized nanoparticle surface. Fig. 3 shows the weight loss of unmodified, silanized and copolymer-anchored Fe_2O_3 nanoparticles, as obtained from TGA measurements. The weight loss of unmodified nanoparticles is related to physisorbed water (between 25 and 150 °C) and surface –OH degradation (between 150 and 850 °C) [27]. For silanized nanoparticles, a significant weight loss starts at around 300 °C, related with silane aminopropil group decomposition [27,29], that was used for the determination of APTS surface density. When the copolymer is anchored to the nanoparticle, different weight loss steps are observed. Besides silane decomposition, thermal decomposition of copolymer can be seen: the decomposition of PCL block occurs in a single step between 200 and 350 °C [30], while main thermal decomposition for PMMA occurs at around 400 and 600 °C [31]. Besides confirming copolymer anchorage, TGA measurements were used to quantify the grafting density of PMMA-*b*-PCL anchored to nanoparticles with the method proposed by Ohno et al. [32]. The highest graft density (0.04 chains/nm^2) was found for 15% copolymer/APTS molar ratio, while the rest of molar ratios used gave lower densities. At this step reaction yield is of around 2%. Nanoparticles with 0.04 chains/nm^2 grafting density were used for nanocomposite preparation. Similar low grafting density values, are usually obtained for *grafting to* process [33], much lower than those obtained for *grafting from*, mainly due to steric hindrance effect [34]. Our group obtained grafting densities of around 0.1 chains/nm^2 for PMMA brushes from Fe_3O_4 nanoparticles [11].

TEM measurements were also used for nanoparticle characterization before and after modification reactions. Fig. 4 shows TEM images of both unmodified and copolymer-grafted nanoparticles. It can be seen that during grafting process nanoparticles tend to aggregate and the modification does not occur around a single nanoparticle but around small aggregates, around which the copolymer can be seen in Fig. 4b. The average size of aggregates is between 20 and 40 nm.

3.4. PS-b-PCL/Fe_2O_3-g-(PMMA-b-PCL) nanocomposite characterization

Morphologies obtained for both copolymer and nanocomposites thin films annealed at 100 and 120 °C have been analyzed by AFM. Fig. 5 shows AFM images of neat block copolymer films annealed at 100 and 120 °C for 72 h. Annealing temperatures are higher than the *Tg* of

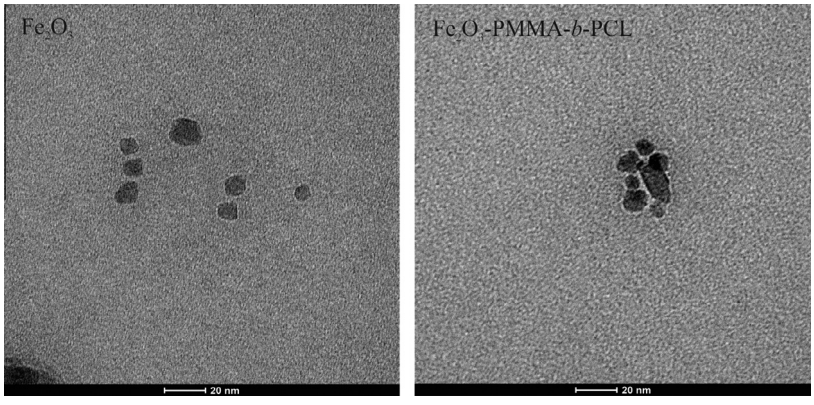

Fig. 4. TEM images of modified and unmodified Fe_2O_3 nanoparticles.

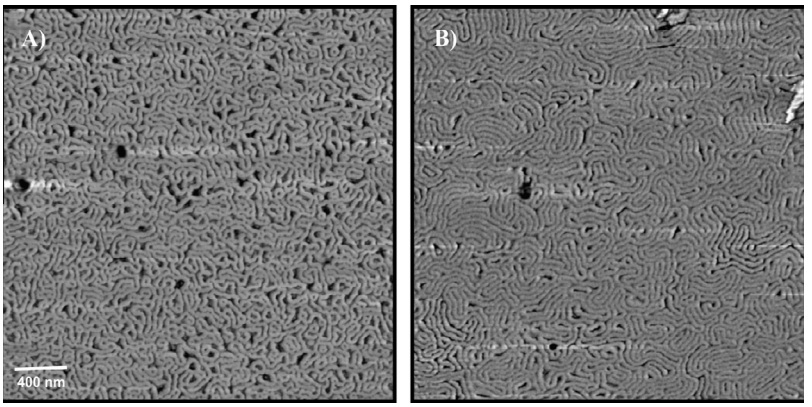

Fig. 5. AFM phase images of PS-*b*-PCL block copolymer annealed for 72 h at: (A) 100 °C and (B) 120 °C.

both blocks, thus allowing chain mobility for nanostructure generation. Films annealed at 100 °C (Fig. 5a) shows worm-like morphology, in which bright domains correspond to PS block, as it is the hardest phase. When annealing temperature is 120 °C (Fig. 5b) a lamellar morphology can be clearly seen. It is worth to note that PCL crystalline domains are not observed in the images. In fact, as it was measured by differential scanning calorimetry (not shown here), crystallization degree of PCL block (only 30% of copolymer) was below 5% in both cases. Furthermore, for nanocomposites crystallization degrees are even lower than 1%.

Fig. 6 shows AFM images of nanocomposites with 2 and 5 wt% of nanoparticles annealed at 100 and 120 °C. As it can be seen the addition of Fe_2O_3 nanoparticles does not modify the morphology of block copolymer. Samples annealed at 100 °C present a worm-like morphology very similar to that of neat copolymer, while those annealed

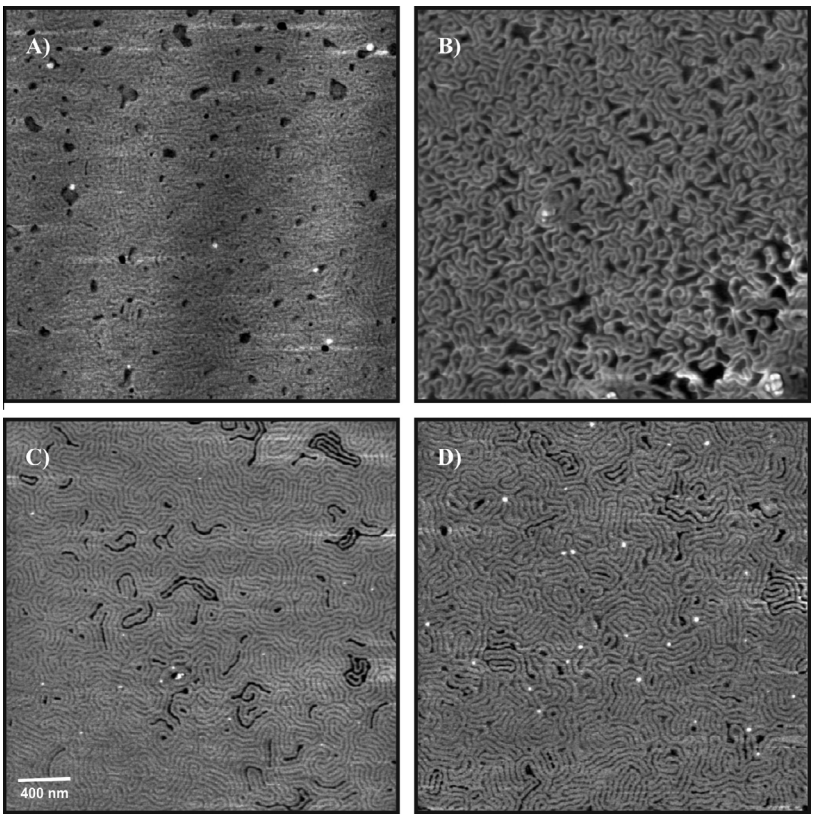

Fig. 6. AFM phase images (3 × 3 μm) of PS-*b*-PCL/Fe_2O_3-*g*-(PMMA-*b*-PCL) nanocomposites annealed at different temperatures and nanoparticle amounts: (A) 100 °C and 2 wt%, (B) 100 °C and 5 wt%, (C) 120 °C and 2 wt% and (D) 120 °C and 5 wt%.

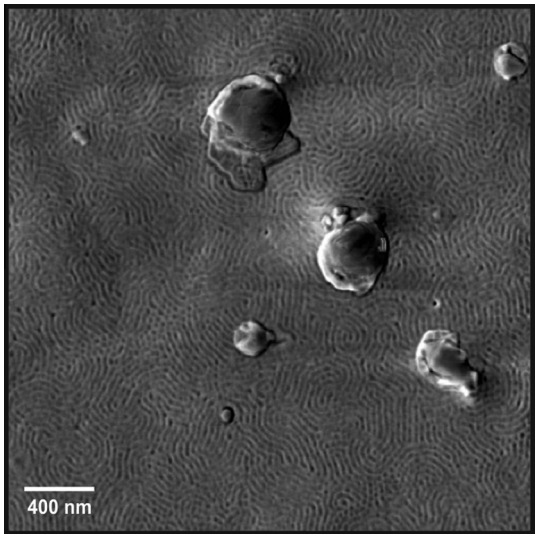

Fig. 7. AFM phase image (3 × 3 μm) of PS-*b*-PCL/Fe_2O_3 nanocomposites with 5 wt% of nanoparticles, annealed at 120 °C for 72 h.

at 120 °C present nanostructured lamellar morphology similarly to neat copolymer. Bright points observed in images of Fig. 6 can be attributed to Fe_2O_3 nanoparticles; the amount of points obviously increases with nanoparticle content. Although small nanoparticle aggregates were formed during grafting process, functionalized nanoparticles are well dispersed in the copolymer. The grafting of nanoparticles with PMMA-*b*-PCL copolymer seems to increase compatibility with copolymer matrix due to the presence of PCL blocks in both, improving dispersion of Fe_2O_3 nanoparticles. For comparison, Fig. 7 shows AFM image of nanocomposite with 5 wt% of unmodified nanoparticles. Bigger aggregates are formed, as nanoparticles tend to aggregate due to their low compatibility with the matrix. It can be seen that surface modification of the nanofillers increased compatibility improving their dispersion. Even if some of them are located in PCL domains, most of Fe_2O_3 nanoparticles grafted with PMMA-*b*-PCL are mainly located at the interface between dark PCL and bright PS domains without altering copolymer nanostructure. Size distribution of Fe_2O_3-*g*-(PMMA-*b*-PCL) in the nanocomposite annealed at 120 °C is shown in Fig. 8 as an example. Average sizes of 22 and 38 nm are obtained for 2 and 5 wt% nanoparticle amount, respectively. Very similar results of 25 and 40 nm are obtained for those nanocomposites annealed at 100 °C. It has to be noted that the size of those aggregates is very similar to that obtained for Fe_2O_3-*g*-(PMMA-*b*-PCL), suggesting that aggregates are formed mainly during modification and not during dispersion in the matrix.

4. Conclusion

Fe_2O_3 nanoparticles have been successfully functionalized, both by silanization and subsequent copolymer grafting, as was demonstrated by FTIR and TGA. This functionalization seems to increase compatibility with copolymer, leading to good nanoparticle dispersion in the nanocomposites, without altering nanostructure generated by block copolymer self-assembly. Nanoparticles are mainly located at the interface between both blocks. During functionalization process, nanoparticles tend to create small aggregates surrounded by copolymer, as it was corroborated by TEM. Those small aggregates are very similar in size that those found in the nanocomposites, suggesting

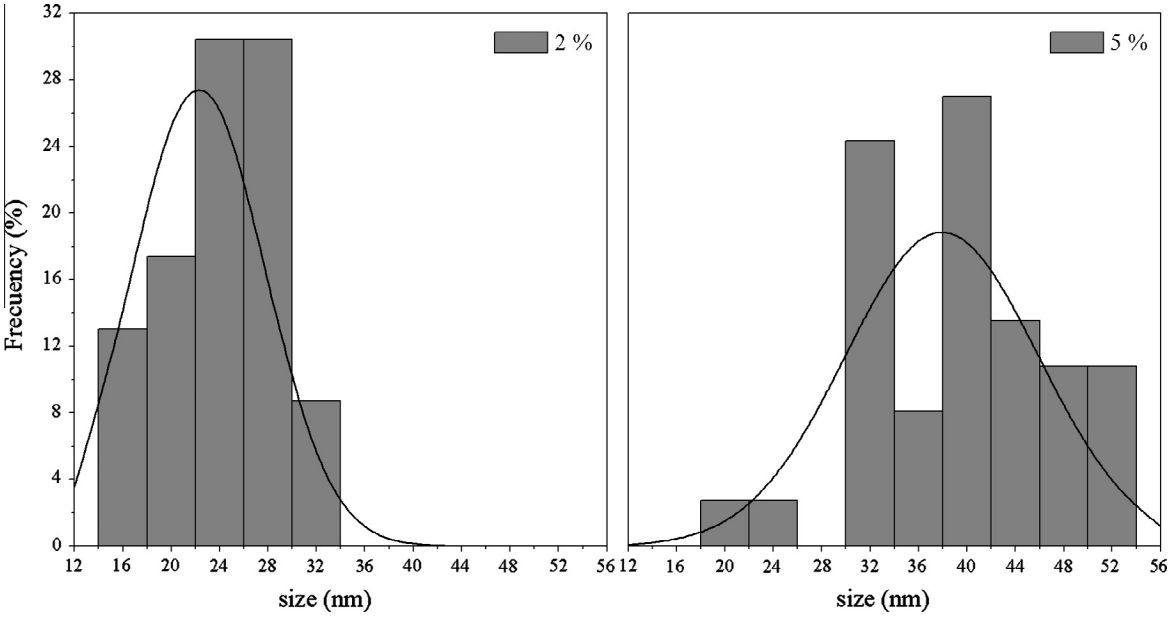

Fig. 8. Fe_2O_3-*g*-(PMMA-*b*-PCL) size distribution in the nanocomposite annealed at 120 °C with: (a) 2 wt% and (b) 5 wt% of nanoparticles.

that dispersion of modified nanoparticles in the copolymer is good, much better than that of unmodified ones.

Acknowledgements

Financial support from the Basque Country Government (Grupos Consolidados, IT-365-07) and the Ministry of Education and Innovation (MAT 2012-31675) is gratefully acknowledged. Technical and human support provided by SGIker. (UPV/EHU, MICINN, GV/EJ, ERDF and ESF) is also acknowledged. I.B. thanks Euskal Herriko Unibertsitatea/Universidad del País Vasco for Ph.D Fellowship (Becas de Formación de Investigadores 2011 (PIF/UPV/11/030)).

References

[1] Stasiaka J, Nair S, Moggridgea GD. Mechanical strength of sutured block copolymers films for load bearing medical applications. Bio-Med Mater Eng 2014;24:563–9. http://dx.doi.org/10.3233/BME-130843.

[2] Endres T, Zheng M, Ķılıç A, Turowska A, Beck-Broichsitter M, Renz, et al. Amphiphilic biodegradable PEG-PCL-PEI triblock copolymers for FRET-capable *in vitro* and *in vivo* delivery of siRNA and quantum dots. Mol Pharmatheutics 2014;3:43. http://dx.doi.org/10.1021/mp400744.

[3] Jia F, Zhang Y, Narasimhan B, Mallapragada SK. Block copolymer-quantum dot micelles for multienzyme colocalization. Langmuir 2012;28:17389–95. http://dx.doi.org/10.1021/la303115t.

[4] Shim JW, Kim S-H, Jeon S-J, Yang S-M, Yi G-R. Microcapsules with tailored nanostructures by microphase separation of block copolymers. Chem Mater 2010;22:5593–600. http://dx.doi.org/10.1021/cm101696t.

[5] García I, Tercjak A, Gutierrez J, Rueda L, Mondragon I. Nanostructuration via solvent vapor exposure of poly(2-vinyl pyridine-*b*-methyl methacrylate) nanocomposites using modified magnetic nanoparticles. J Phys Chem 2008;112:14343–7. http://dx.doi.org/10.1021/jp802345q.

[6] Gutierrez J, Tercjak A, Garcia I, Mondragon I. The effect of thermal and vapor annealing treatments on the self-assembly of TiO_2/PS-*b*-PMMA nanocomposites generated via the sol–gel process. Nanotechnology 2009;20:225603. http://dx.doi.org/10.1088/0957-4484/20/22/225603.

[7] Etxeberria H, Zalakain I, Fernandez R, Kortaberria G, Mondragon I. Controlled placement of polystyrene-grafted CdSe nanoparticles in self-assembled block copolymers. Colloid Polym Sci 2013;291:633–40. http://dx.doi.org/10.1007/s00396-012-2765-0.

[8] Lopes WA, Jaeger HM. Hierarchical self-assembly of metal nanostructures on diblock copolymer scaffolds. Nature 2001;414:735–8. http://dx.doi.org/10.1038/414735a.

[9] Cheng JY, Ross CA, Chan VZ-H, Thomas EL, Lammertink RGH, Vancso GJ. Formation of a cobalt magnetic dot array via block copolymer lithography. Adv Mater 2001;13:1174–8. 0935-9648/01/1508-1174.

[10] Ouk Kim S, Solak HH, Stoykovich MP, Ferrier NJ, de Pablo JJ, Nealey PF. Epitaxial self-assembly of block copolymers on lithographically defined nanopatterned substrates. Nature 2003;424:411–4. http://dx.doi.org/10.1038/nature0177.

[11] García I, Zafeiropoulos NE, Janke A, Tercjak A, Eceiza A, Stamm M, et al. Functionalization of iron oxide magnetic nanoparticles with poly(methyl methacrylate) brushes via grafting-from atom transfer radical polymerization. J Polym Sci Part A: Polym Chem 2007;45:925–32. http://dx.doi.org/10.1002/pola.21854.

[12] Kondo A, Fukuda H. Preparation of thermo-sensitive magnetic microspheres and their application to bioprocesses. Colloids Surf A 1999;155:435–8. S0927-7757(98)00465-8.

[13] Hsiao J, Taic M, Leed Y, Yanga C, Wangd H, Liua H, et al. Labelling of cultured macrophages with novel magnetic nanoparticles. Magn Magn Mater 2006;304:e4–6. http://dx.doi.org/10.1016/j.jmmm.2006.01.134.

[14] Shen H, Long D, Zhu L, Li X, Dong Y, Jia N, et al. Magnetic force microscopy analysis of apoptosis of HL-60 cells induced by complex of antisense oligonucleotides and magnetic nanoparticles. Biophys Chem 2006;122:1–4. http://dx.doi.org/10.1016/j.bpc.2006.01.003.

[15] Peponi L, Tercjak A, Torre L, Kenny JM, Mondragon I. Surfactant effects on morphology-properties relationships of silver-poly(styrene-b-isoprene-b-styrene) block copolymer nanocomposites. J Nanosci Nanotechnol 2009;9:2128–39. http://dx.doi.org/10.1166/jnn.2009.43.

[16] Etxeberria H, Zalakain I, Mondragon I, Eceiza A, Kortaberria G. Generation of nanocomposites based on polystyrene-grafted CdSe nanoparticles by grafting through and block copolymer. Colloid Polym Sci 2013;291:1881–6. http://dx.doi.org/10.1007/s00396-013-2927-8.

[17] Minko S, Patil S, Datsyuk V, Simon F, Eichchorn K, Motornov M, et al. Synthesis of adaptive polymer brushes via "grafting to" approach from melt. Langmuir 2002;18:289–96. http://dx.doi.org/10.1021/la015637q.

[18] Trabelsi S, Janke A, Häßler R, Zafeiropoulos NE, Stamm M, Fornasieri G, et al. Novel organo-functional titanium–oxo-cluster-based hybrid materials with enhanced thermomechanical and thermal properties. Macromolecules 2002;35:4960–7. http://dx.doi.org/10.1021/ma0507239.

[19] Wang S, Zhou Y, Guan W, Ding B. One-step copolymerization modified magnetic nanoparticles via surface chain transfer free radical polymerization. Appl Surf Sci 2008;254:5170–4. http://dx.doi.org/10.1016/j.apsusc.2008.02.021.

[20] Zhou Y, Wang S, Ding B, Yang Z. Modification of magnetite nanoparticles via surface-initiated atom transfer radical polymerization (ATRP). Chem Eng J 2008;138:578–85. http://dx.doi.org/10.1016/j.cej.2007.07.030.

[21] He X, Wu X, Cai X, Lin S, Xie M, Zhu X, et al. Functionalization of magnetic nanoparticles with dendritic–linear–brush-like triblock copolymers and their drug release properties. Langmuir 2012;28:11929–38. http://dx.doi.org/10.1021/la302546m.

[22] Zhang X, Matyjaszewski K. Synthesis of well-defined amphiphilic block copolymers with 2-(dimethylamino)ethyl methacrylate by controlled radical polymerization. Macromolecules 1999;32:1763–6. http://dx.doi.org/10.1021/ma981332f.

[23] Abbound M, Turner M, Duguet E, Fontanille M. PMMA-based composite materials with reactive ceramic fillers. Part 1. Chemical modification and characterization of nanoparticles. J Mater Chem 1997;7:1527–32. http://dx.doi.org/10.1039/A700573.

[24] Jing Z. Preparation and magnetic properties of fibrous gamma iron oxide nanoparticles via nonaqueous medium. Mater Lett 2006;60:2217–21. http://dx.doi.org/10.1016/j.matlet.2005.12.109.

[25] Wang C, Ro S. Nanoparticle iron–titanium oxide aerogels. Mater Chem Phys 2007;101:41–8. http://dx.doi.org/10.1016/j.matchemphys.2006.02.010.

[26] Marutani E, Yamamoto S, Ninjbadgar T, Tjii Y, Fukuda T, Takano M. Surface initiated atom transfer radical polymerization of methyl methacrylate on magnetic nanoparticles. Polymer 2004;45:2231–5. http://dx.doi.org/10.1016/j.polymer.2004.02.005.

[27] Cosio-Castañeda C, Martinez-Garcia R, Socolovsky LM. Synthesis of silanized maghemite nanoparticles onto reduced graphene sheets composites. Solid State Sci 2014;30:17–20. http://dx.doi.org/10.1016/j.solidstatesciences.2014.02.004.

[29] Galeotti F, Bertini F, Scavia G, Bolognesi A. A controlled approach to iron oxide nanoparticles functionalization for magnetic polymer brushes. J Colloid Interface Sci 2011;360:540–7. http://dx.doi.org/10.1016/j.jcis.2011.04.076.

[30] Rana S, Yoo HJ, Cho JW, Chun BC, Park JS. Functionalization of multi-walled carbon nanotubes with poly(ε-caprolactone) using click chemistry. J Appl Polym Sci 2011;119:31–7. http://dx.doi.org/10.1002/app.31268.

[31] Ferriol M, Gentilhomme A, Cochez M, Oget N, Mieloszynski JL. Thermal degradation of poly(methyl methacrylate) (PMMA): modelling of DTG and TG curves. Polym Degrad Stab 2003;79:271–81. http://dx.doi.org/10.1016/S0141-3910(02)00291-4.

[32] Ohno K, Koh K, Tsuji Y, Fukuda T. Synthesis of gold nanoparticles coated with well-defined, high density polymer brushes by surface-initiated living radical polymerization. Macromolecules 2002;35:8989. http://dx.doi.org/10.1021/ma0209491.

[33] Minko S, Patil S, Datsyuk V, Simon F, Eichhorn KJ, Motornov M, et al. Synthesis of polymer brushes via grafting to approach. Langmuir 2002;18:289–96. http://dx.doi.org/10.1021/la015637q.

[34] Mansky P, Liu Y, Huang E, Russel TP, Hawker C. Controlling polymer-surface interactions with random copolymer brushes. Science 1997;275:1458–60. http://dx.doi.org/10.1126/science.275.5305.1458.